PNAS
www.pnas.org

Supplementary Information for:

Cognitive impairment after focal brain lesions is better predicted by damage to structural than functional network hubs

Justin Reber, PhD [a,b *]
Kai Hwang, PhD [c]
Mark Bowren, MA [b,c]
Joel Bruss, BA [b]
Pratik Mukherjee, MD, PhD [d]
Daniel Tranel, PhD [b, c]
Aaron D. Boes, MD, PhD [a,b,e]

[a] Department of Psychiatry, Carver College of Medicine, Iowa City, IA 52242;
[b] Department of Neurology (Division of Neuropsychology and Cognitive Neuroscience), Carver College of Medicine; Iowa City, IA, 52242;
[c] Department of Psychological and Brain Sciences; University of Iowa; Iowa City, IA, 52242;
[d] Department of Radiology and Bioengineering, University of California, San Francisco, CA, 94143;
[e] Department of Pediatrics, Carver College of Medicine, Iowa City, IA 52242

*Send correspondence to:
Justin Reber, PhD
Iowa Neuroimaging & Noninvasive Brain Stimulation Laboratory
Department of Psychiatry
University of Iowa Hospitals and Clinics
W276 GH, 200 Hawkins Drive, Iowa City, IA 52242
Phone: 319-353-8587
Email: justin-reber@uiowa.edu

This PDF file includes:

Supplementary Methods

Derivation of estimates of general cognitive ability. General cognitive performance was derived from the neuropsychological tests most commonly administered to the participants in the Iowa cohort (Table S7). Each test was assigned to latent variables using the Cattell-Horn-Carroll (CHC) model of cognitive abilities (1), a widely used taxonomy of mental abilities that robustly accounts for the covariance structure of the neuropsychological tests administered to these patients (2). Several of these tests are subtests of the Wechsler Adult Intelligence Scale (WAIS), the most widely-used assessment for measuring multiple facets of intelligence, which has extensive psychometric literature supporting both its reliability and validity (3). All subjects were administered the most up-to-date version of the WAIS at the time of their assessment. When a patient had more than one score on an assessment, we used the administration most contemporaneous with the date of the patient's chronic epoch MRI scan. Test scores were adjusted for age using normative data from test manuals, meta-normative data, or normative data from the Benton Neuropsychology Laboratory (3-5). All age-adjusted scores were transformed into standard units (i.e., Z-scores). In instances where test scores were omitted, these data were imputed using multiple imputation by chained equations as implemented in the MICE package (6) available in R (7). 5% of the total dataset was imputed.

Structural equation models were used to measure the association between each specific cognitive ability and general cognition using the Iowa data. We used a structural equation modeling framework over an exploratory approach whenever possible because of the greater hypothesis-testing flexibility afforded by the former, especially as it relates

to bifactor modeling (8, 9), and because previous work has evaluated how the Iowa neuropsychological tests fit into the architecture of the CHC model (2). These analyses were performed using the lavaan library in R (10). All free parameters were estimated using maximum likelihood. Parameters were reported from the completely standardized solutions (i.e., all factor loadings were standardized between values of 0 and 1). Standard errors for all parameters were derived using the bootstrapping procedures (with 1000 draws) available in the structural equation model (sem) function in lavaan. For each model, local fit was inspected to identify parameters that were not statistically significantly different from zero. Overall model fit to the data was evaluated using the Comparative Fit Index (CFI), the Root Mean Square Error of Approximation (RMSEA), and the standardized root mean square residual (SRMR). Acceptable model fit is indicated by CFI of at least 0.90, and RMSEA and SRMR less than or equal to 0.08 (11). Scores for latent variables were generated using the lavPredict function in R, which estimates values of latent variables using a regression based on model parameters.

The following domain-specific cognitive abilities could be modeled from the observed data: crystallized intelligence, visuospatial ability, learning efficiency, processing speed, and working memory. To account for method covariance, the unique variances of the Complex Figure Test Copy and Recall scores were allowed to covary in all models, as were the unique variances of parts A and B of the Trail Making Test, and the indices of the Rey Auditory Verbal Learning Test. A hierarchical model was used to estimate g and to examine the variance in g that can be accounted for by each domain-specific ability. The square of the correlation between each ability and g served as an index of the

variance in g explained by each specific cognitive ability; this is indicated by the factor loading of each ability on g (12).

Peak within the lesion. In addition to the pre-registered lesion load analyses, we also considered an alternative method of quantifying the overlap of lesions onto network maps that was less dependent on lesion volume. Lesion load, used for the main analysis, was a summation of all voxel values within the entire lesion volume, and thus larger lesions had more voxels included and had higher lesion load values, on average. Thus, widespread damage to low-importance regions would appear quantitatively equivalent to a smaller lesion to a hub region, although the impact on cognition may differ. For this analysis, we rank-ordered the voxels in each individual lesion by their edge density values, then we took the average edge density value of the top 100 voxels, corresponding to a volume of 800 mm^3 (about the size of the hypothalamus, for reference). This represents a volume smaller than most lesions, yet large enough to identify regional peaks within lesions. This process was repeated with participation coefficient.

We repeated the same regression models (models 1-3), replacing lesion load with "lesion peak" values. Overall, these models were similar to the main analyses and predicted more overall variance. Lesion volume was again used in step 1. In the first model, edge density "lesion peak" was a significant predictor of cognitive impairment, (model 1, step 2: β=-0.220, ΔR^2=0.033, p<0.001). Participation coefficient "lesion peak," however, was not significantly associated with impairment, (model 2, step 2: β=0.003, ΔR^2=0.000, p=.971). In model 3, combining both "lesion peak" measures explained significantly more variance in cognitive performance than lesion volume alone, (model 3, step 2: ΔR^2=0.033, p=.001). Similar to the combined lesion load regression models, "lesion peak" edge density was negatively associated with g (β=-0.220, p<.001), but

"lesion peak" participation coefficient did not have a significant association with *g* (β=-0.007, p=.932). These results are presented in Table 1 of the main text.

Controlling for pre-morbid differences in cognition. We presume that some of the variance in post-lesion cognitive ability is explained by pre-morbid differences. While there is no perfect way to account for such differences in a study of human participants with naturally-occurring lesions that preceded their involvement in research, we attempted to estimate pre-morbid cognitive differences using an aggregate crystallized intelligence score calculated from three assessments—the WAIS Similarities subtest, WAIS Information subtest, and the Wide Range Achievement Test (WRAT) Word Reading subtest—as an estimate of pre-morbid cognitive ability (13, 14). Using this crystallized intelligence score, we calculated a new residualized *g* score with the effect of crystallized intelligence regressed out. We then re-ran our analyses on these residual values (Table 1). In the overall model containing lesion volume, edge density lesion load, and participation coefficient lesion load, lesion volume significantly predicted cognitive ability (β=-0.255, p<0.001). The second step of the regression with both edge density and participation coefficient lesion load added a significant improvement in predictive variance over total lesion volume, (p<0.001, ΔR^2=0.069). Just as in previous models, total edge density lesion load was significantly associated with cognitive ability, (β=-0.256, p=.007). Participation coefficient lesion load, on the other hand, was not significantly predictive of post-lesion cognitive ability, (β=-0.138, p=.154).

Peak hub in the brain. We also investigated whether lesions that occur at the locations in the brain with the highest overall edge density and highest participation coefficient were associated with impaired cognition. To test this, we identified the regions with the highest overall edge density and participation coefficient in the brain and divided patients into two groups: individuals whose lesions damaged this peak hub region, and individuals without damage to those voxels. The average *g* score of both groups were compared. For edge density, the peak was MNI coordinate (-37, -43, 3). The difference in average *g* score between patients who had damage to this high edge density region and patients who did not were marked (*N*=11, *mean g*=-0.604 compared to *N*=391; *mean g*=0.017, *t*(400)= 2.221, *p*=.027). On the other hand, the group with damage to the highest participation coefficient regions—which included the midline cerebellum (2, -62, -24), thalamus (9, -4, 8), and precuneus (-6, -62, 56)—did not show significant differences from those with lesions that did not damage those regions, (*N*=5, *M*=-0.692 compared to *N*=397, *M*=-0.009, *t*(400)=1.698, *p*=.090).

A more systematic test comparing differences in cognitive performance between groups using a sliding-scale threshold for each map produced similar results, both in the Iowa and WU cohorts. In this analysis, we wanted to investigate whether the regions of the brain with the overall highest network importance based on participation coefficient or edge density were associated with the greatest deficits in cognitive performance when lesioned. To address this question, we applied a progressively more stringent threshold to the edge density and participation coefficient maps and evaluated the cognitive performance of subjects with lesions that intersect with these maps, which resulted in a progressively smaller number of subjects having lesions that overlap with the maps as the

threshold is increased. We were then able to evaluate whether those subjects with lesions that intersect with regions with maximum participation coefficient and edge density across the entire brain have greater cognitive impairment. For the edge density white matter map there was a peak voxel intensity of 42.076, and we generated maps ranging from no threshold applied to a threshold in which only the peak voxels in the brain were included, with everything in between in graded steps (0, 1, 2, 3… to 42). Similarly, for participation coefficient there was a range of voxel intensities from 0 to a peak participation coefficient value of 0.789. We applied a similar progressively more stringent threshold gradation, with the minimum value increasing from 0 by 0.0197 (the maximum intensity divided by 40).

At each threshold, patients were divided into two groups: individuals whose lesions damaged nonzero voxels on the map, and individuals without damage to those voxels (Figure S1). The average *g* score of both groups were then plotted (Figure S2a). All patients had lesions overlapping the edge density map at the 0 threshold, and that number decreased until only 11 patients overlapped the voxels with the highest edge density values of anywhere in the brain, with a threshold of 42 at MNI coordinates [-37.08, -43.16, 3.98] (Figure S2b). For participation coefficient, all but four patients had lesions overlapping the participation coefficient map until the 0.5325 threshold, and only one patient had damage to a non-zero participation coefficient region— located in the midline cerebellum centered at MNI coordinates [2.67 -62.99 -32.48]—at the final 0.7889 threshold (Figure S3). Notably, the difference in average *g* score between patients who had damage to high edge density regions and patients who did not were marked, and appeared to increase progressively when thresholds were applied above edge density of

34. On the other hand, the difference between groups with damage to high participation coefficient regions did not show similar increases with a progressively more stringent threshold. A similar pattern was present in the WU cohort—the average cognitive performance was lower for patients with lesions overlapping high edge density regions, but not high participation coefficient, regions (Figure S4).

Sex differences. We divided the Iowa cohort into men and women and re-ran our primary analyses to evaluate the potential role of sex differences in these relationships. The pattern of results remained the same in the men (N=211), but for the women (N=190), neither edge density load nor participation coefficient were significant predictors of g in the second step of the model. Despite these differences observed when splitting the cohort by sex, we did not observe a significant interaction between sex and edge density lesion load or participation coefficient lesion load. More research is needed to determine whether the different significance levels in men and not women is due to an under-powered analysis or another combination of factors.

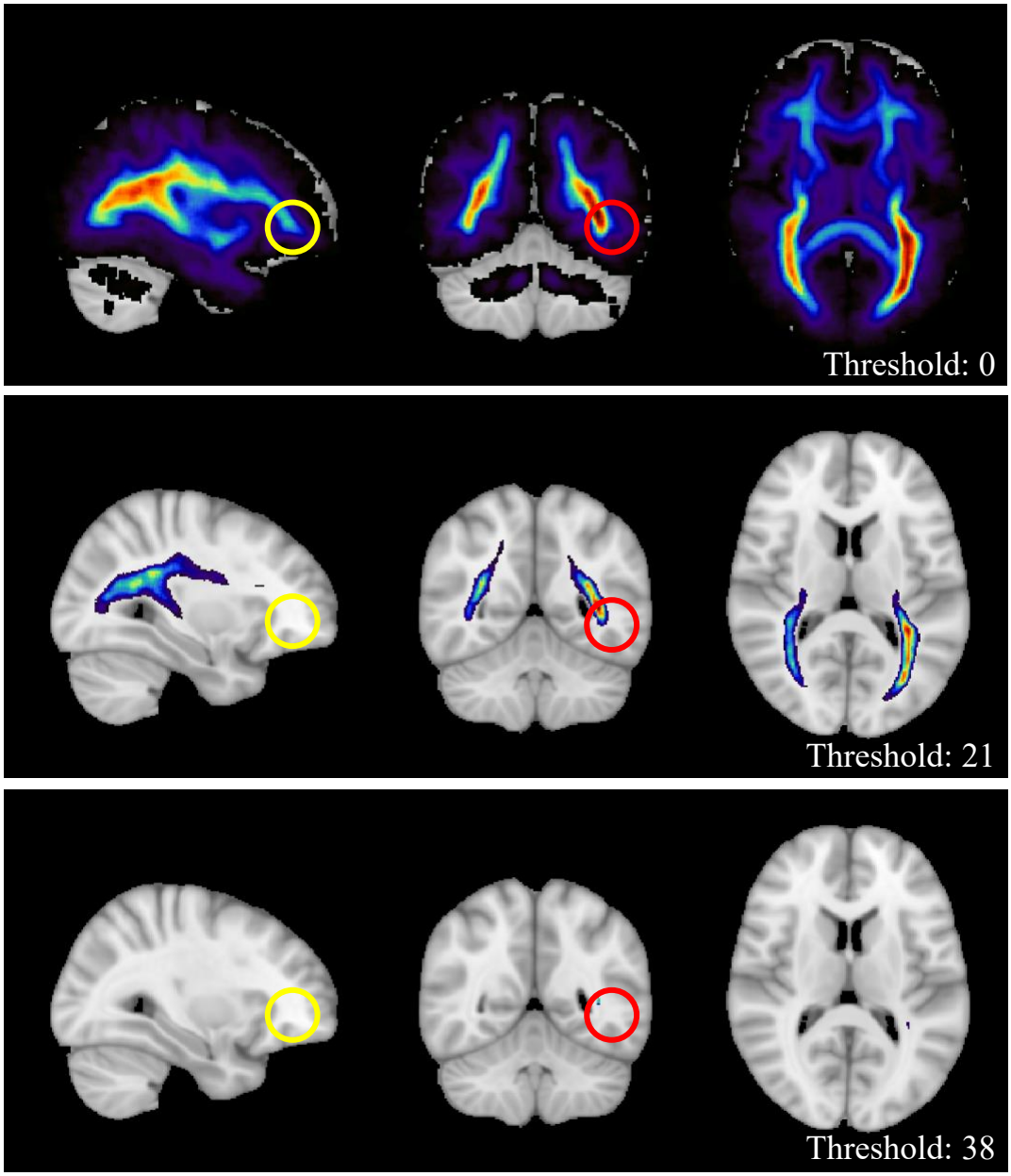

Figure S1. Increasing the minimum threshold for edge density. A patient with a lesion to the region in the yellow circle would overlap the edge density map at a threshold of 0, but not at 21 or 38. A patient with a lesion in the red circle region, however, would overlap an edge density "hub" at all three threshold levels.

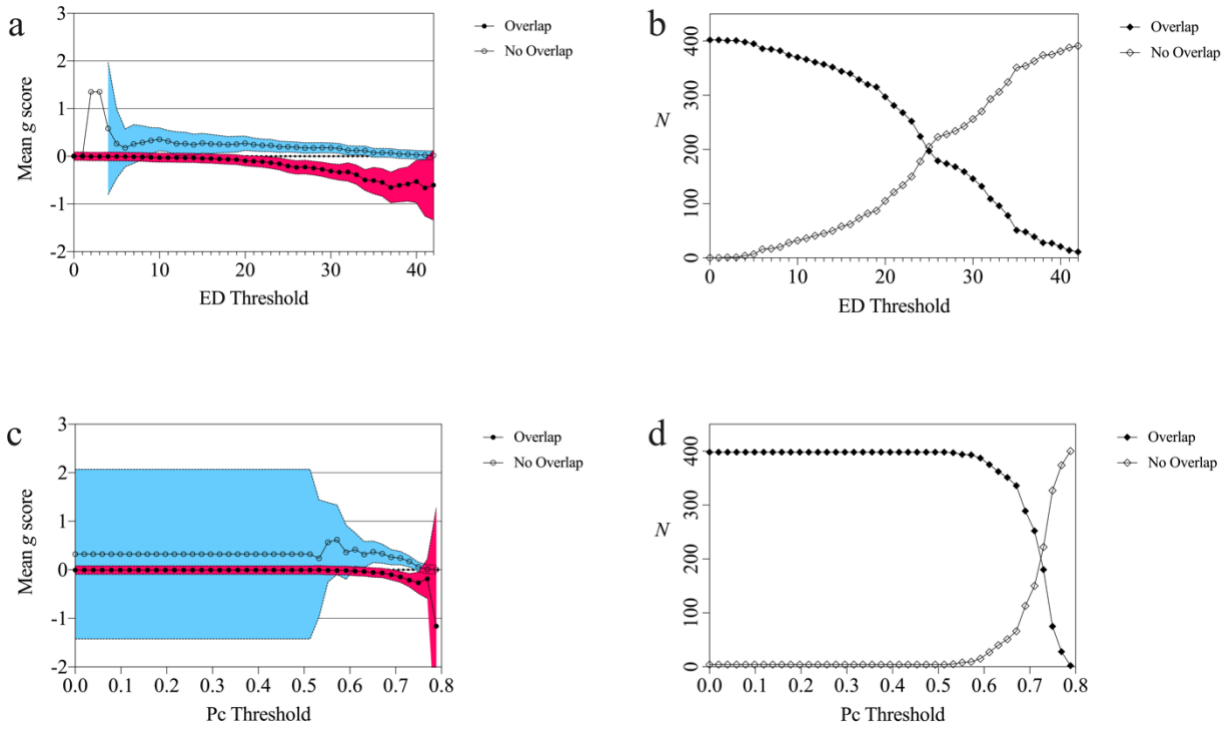

Figure S2. Mean *g* score and group *N* for threshold analyses of the Iowa cohort. Colored areas in **(a)** and **(c)** represent 95% confidence intervals. ED = Edge density, Pc = Participation coefficient. **(a)** The average *g* score of the group with damage to regions with non-zero edge density dropped considerably as the threshold increased. **(b & d)** The number of patients with lesions overlapping areas with non-zero edge density and participation coefficient decreased as the edge density and participation coefficient thresholds respectively increased.

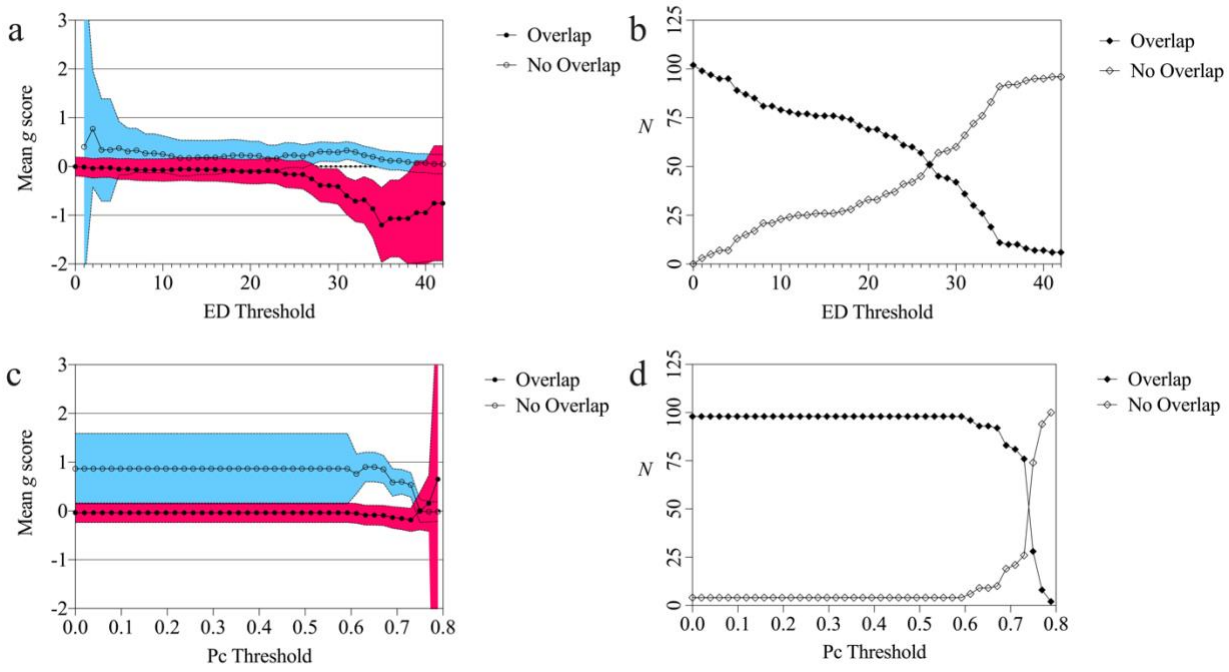

Figure S3. Mean *g* score and group *N* for threshold analyses of the WU cohort. Colored areas in **(a)** and **(c)** represent 95% confidence intervals. ED = Edge density, Pc = Participation coefficient. **(a)** Similar to the Iowa cohort, the average *g* score of the group with damage to regions with non-zero edge density dropped considerably as the threshold increased. **(b & d)** The number of patients with lesions overlapping areas with non-zero edge density and participation coefficient decreased as the edge density and participation coefficient thresholds respectively increased.

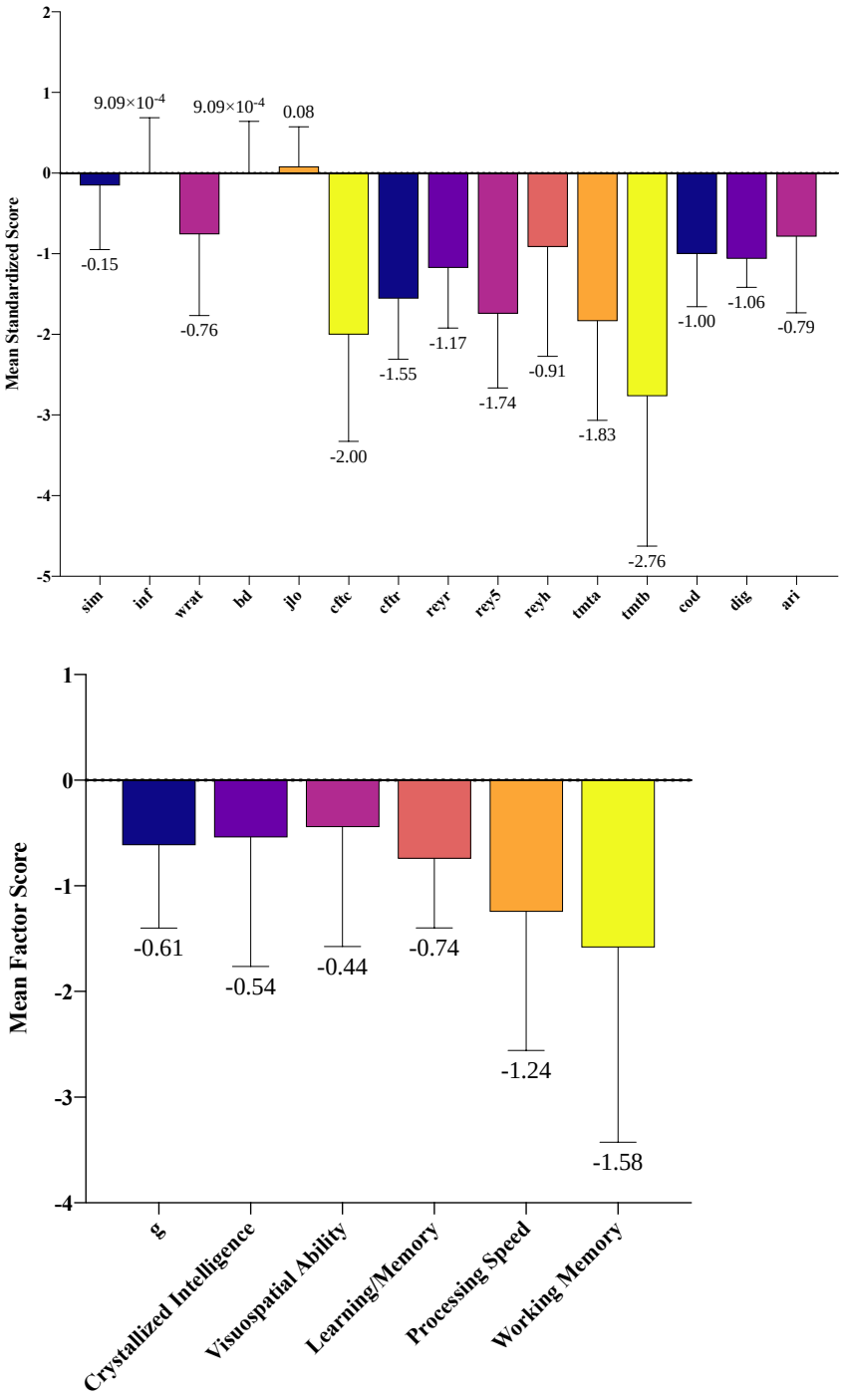

Figure S4. (a) Mean standardized assessment scores and **(b)** factor scores for eleven individuals from the Iowa cohort with lesions overlapping the highest edge density threshold.

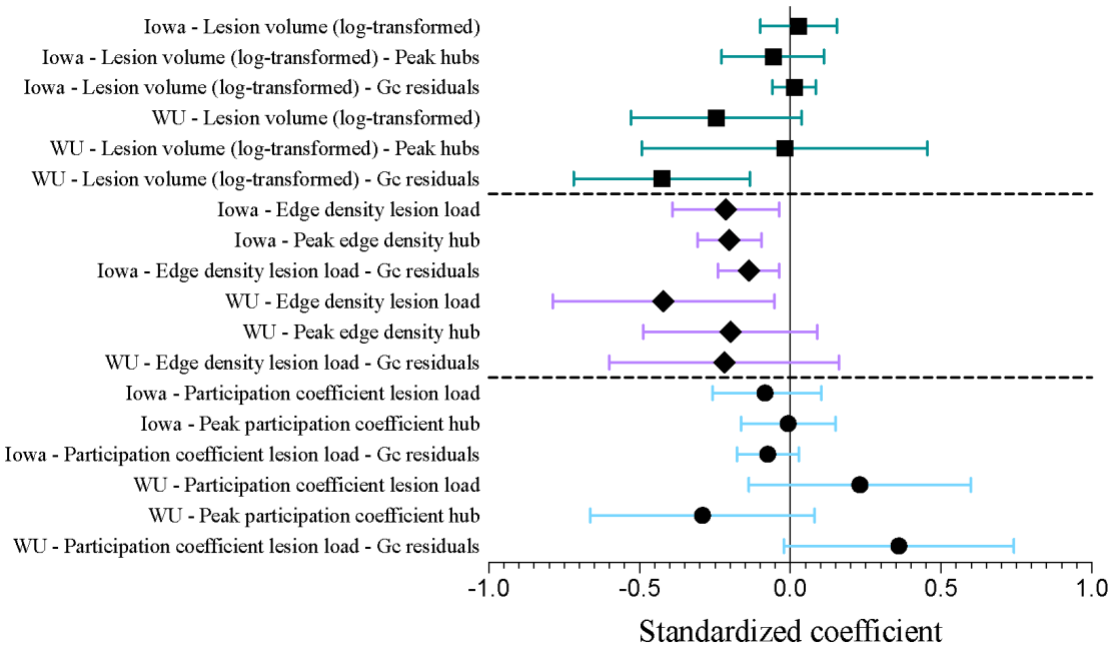

Figure S5. Main regression coefficients. Standardized regression coefficients for the predictor variables for all primary models in both cohorts. Both lesion volume and participation coefficient do not have a consistent relationship with cognitive impairment, but the edge density of lesions, whether it was the peak cluster within the lesion or the overall lesion load, had a consistently negative relationship with cognition, both uncorrected and corrected for crystallized intelligence (Gc residuals). Error bars represent 95% confidence intervals.

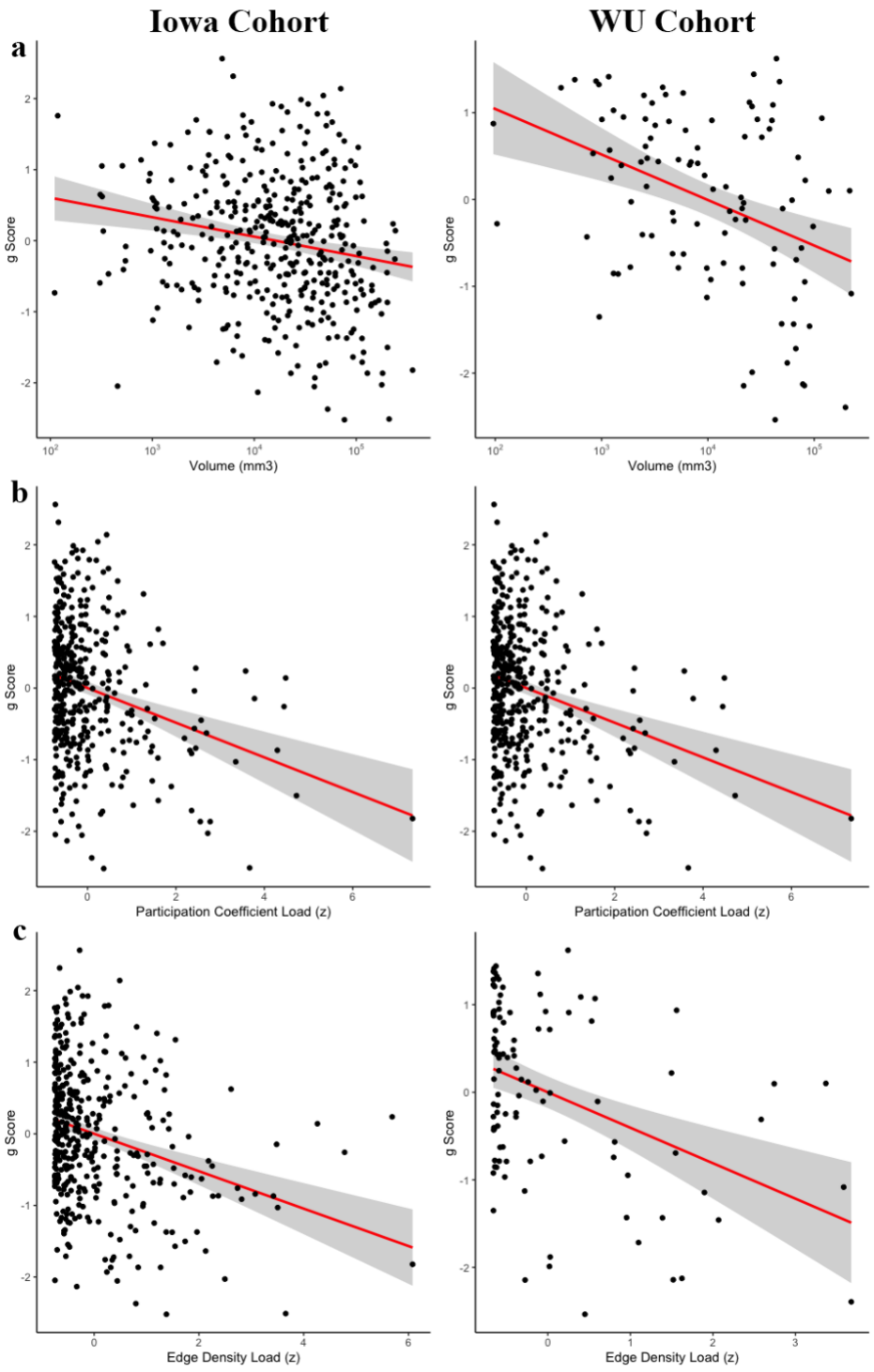

Figure S6. Scatterplots of primary variables in both the Iowa (N=402) and WU (N=102) cohorts.

Table S1.

Iowa Cohort: Hierarchical Linear Regressions with Lesion Volume, Edge Density Load, and Participation Coefficient Load Predicting Post-Lesion g Scores

	Step and Variable	*b*	95% CI for *b* Lower bound	95% CI for *b* Upper bound	β	*t*	*p*	*df*	R^2	ΔR^2	Sig. ΔF	AIC
Model 1	Step 1											
	Total Lesion Volume (mm^3)	**0.000**	**0.000**	**0.000**	**-0.256**	**-5.300**	**<.001**	**400**	**0.066**	**0.066**	**<.001**	**-92.087**
	Step 2											
	Total Lesion Volume (mm^3)	0.000	0.000	0.000	0.508	1.960	.051	398	0.084	0.025	.004	-99.114
	Edge Density Load	**-0.351**	**-0.576**	**-0.126**	**-0.382**	**-3.063**	**.002**	**398**	**0.084**	**0.025**	**.004**	**-99.114**
	Participation Coefficient Load	**-0.392**	**-0.762**	**-0.022**	**-0.427**	**-2.085**	**.038**	**398**	**0.084**	**0.025**	**.004**	**-99.114**
Model 2	Step 1											
	Total Lesion Volume (mm^3)	**0.000**	**0.000**	**0.000**	**-0.256**	**-5.260**	**<.001**	**396**	**0.063**	**0.065**	**<.001**	**-91.797**
	Step 2											
	Total Lesion Volume (mm^3)	0.000	0.000	0.000	-0.004	-0.019	.985	395	0.065	0.004	.194	-91.497
	Participation Coefficient Load	-0.238	-0.597	0.122	-0.260	-1.300	.194	395	0.065	0.004	.194	-91.497
Model 3	Step 1											
	Total Lesion Volume (mm^3)	**0.000**	**0.000**	**0.000**	**-0.256**	**-5.300**	**<.001**	**400**	**0.066**	**0.066**	**<.001**	**-92.087**
	Step 2											
	Total Lesion Volume (mm^3)	0.000	0.000	0.000	0.029	0.240	.810	399	0.081	0.015	.010	-96.748
	Edge Density Load	**-0.286**	**-0.503**	**-0.068**	**-0.311**	**-2.582**	**.010**	**399**	**0.081**	**0.015**	**.010**	**-96.748**

Note: R^2 represents adjusted R^2. AIC = Akaike Information Criterion. Variable Inflation Factors for predictor variables ranged between 6.8 and 29.4, so models should be interpreted with caution. Four patients had lesions that did not intersect with the participation coefficient map and were thus excluded from Model 2 (N=402).

Table S2.

WU Cohort: Hierarchical Linear Regressions with Lesion Volume, Edge Density Load, and Participation Coefficient Load Predicting Post-Lesion g Scores

	Step and Variable	*b*	95% CI for *b* Lower bound	95% CI for *b* Upper bound	β	*t*	*p*	*df*	R^2	ΔR^2	Sig. ΔF	AIC
Model 1	Step 1											
	Total Lesion Volume (mm^3)	**0.000**	**0.000**	**0.000**	**-0.350**	**-3.740**	**<.001**	**100**	**0.114**	**0.123**	**<.001**	**-10.360**
	Step 2											
	Total Lesion Volume (mm^3)	0.000	0.000	0.000	0.604	0.776	.439	98	0.123	0.051	.053	-12.476
	Edge Density Load	-0.761	-1.476	-0.046	-0.761	-2.112	.037	98	0.123	0.051	.053	-12.476
	Participation Coefficient Load	-0.247	-1.277	0.783	-0.247	-0.476	.635	98	0.123	0.051	.053	-12.476
Model 2	Step 1											
	Total Lesion Volume (mm^3)	**0.000**	**0.000**	**0.000**	**-0.336**	**-3.496**	**.001**	**96**	**0.104**	**0.113**	**.001**	**-8.499**
	Step 2											
	Total Lesion Volume (mm^3)	0.000	0.000	0.000	-0.838	-2.104	.038	95	0.110	0.015	.197	-8.222
	Participation Coefficient Load	0.513	-0.271	1.297	0.517	1.298	.197	95	0.110	0.015	.197	-8.222
Model 3	Step 1											
	Total Lesion Volume (mm^3)	**0.000**	**0.000**	**0.000**	**-0.350**	**-3.740**	**<.001**	**100**	**0.114**	**0.123**	**<.001**	**-10.360**
	Step 2											
	Total Lesion Volume (mm^3)	0.000	0.000	0.000	0.256	0.962	.338	99	0.155	0.049	.017	-14.240
	Edge Density Load	**-0.646**	**-1.175**	**-0.117**	**-0.646**	**-2.424**	**.017**	**99**	**0.155**	**0.049**	**.017**	**-14.240**

Note: R^2 represents adjusted R^2. AIC = Akaike Information Criterion. Variable Inflation Factors for predictor variables ranged between 15.4 and 71.8, so models should be interpreted with caution.

Table S3.

Predicting Post-Lesion g Scores in WU Cohort

Predictors	*r*	*p*	*df*	*RMSE*
Total Lesion Volume (log mm^3)	0.386	<.001	102	0.938
Model 1 - Total Lesion Volume (log mm^3) + Edge Density Load + Participation Coefficient	0.380	<.001	102	0.928
Model 2 - Total Lesion Volume (log mm^3) + Participation Coefficient	0.329	.001	102	0.958
Model 3 - Total Lesion Volume (log mm^3) + Edge Density Load	0.401	<.001	102	0.922
Total Lesion Volume (log mm^3) + Lesion Peak Edge Density + Lesion Peak Participation Coefficient	0.341	<.001	102	0.938

RMSE = Root Mean Squared Error.

Table S4.

Iowa Cohort: Hierarchical Linear Regressions with Log-Transformed Lesion Volume, Edge Density Load, and Three Alternative Calculations of Participation Coefficient Load Predicting Post-Lesion g Scores

	Step and Variable	*b*	95% CI for *b* Lower bound	95% CI for *b* Upper bound	β	*t*	*p*	*df*	R^2	ΔR^2	Sig. ΔF	AIC
Reparcellation	Step 1											
	Total Lesion Volume (log mm^3)	**-0.118**	**-0.178**	**-0.058**	**-0.191**	**-3.867**	**<.001**	**395**	**0.034**	**0.036**	**<.001**	**-78.712**
	Step 2											
	Total Lesion Volume (log mm^3)	0.018	-0.071	0.106	0.029	0.391	.696	393	0.074	0.044	<.001	-93.360
	Edge Density Load	**-0.233**	**-0.407**	**-0.060**	**-0.254**	**-2.641**	**.009**	**393**	**0.074**	**0.044**	**<.001**	**-93.360**
	Participation Coefficient Load - Yeo Parcellation	-0.053	-0.238	0.132	-0.057	-0.561	.575	393	0.074	0.044	<.001	-93.360
Alternative rs-fMRI dataset (HCP)	Step 1											
	Total Lesion Volume (log mm^3)	**-0.118**	**-0.178**	**-0.058**	**-0.191**	**-3.867**	**<.001**	**395**	**0.034**	**0.036**	**<.001**	**-78.712**
	Step 2											
	Total Lesion Volume (log mm^3)	0.013	-0.074	0.099	0.020	0.286	.775	393	0.073	0.044	<.001	-93.135
	Edge Density Load	**-0.249**	**-0.427**	**-0.071**	**-0.270**	**-2.750**	**.006**	**393**	**0.073**	**0.044**	**<.001**	**-93.135**
	Participation Coefficient Load - HCP Dataset	-0.028	-0.212	0.156	-0.031	-0.303	.762	393	0.073	0.044	<.001	-93.135
Alternative rs-fMRI dataset (NKI)	Step 1											
	Total Lesion Volume (log mm^3)	**-0.118**	**-0.178**	**-0.058**	**-0.191**	**-3.867**	**<.001**	**395**	**0.034**	**0.036**	**<.001**	**-78.712**
	Step 2											
	Total Lesion Volume (log mm^3)	0.021	-0.065	0.107	0.034	0.480	.632	393	0.075	0.046	<.001	-94.067
	Edge Density Load	**-0.200**	**-0.382**	**-0.018**	**-0.217**	**-2.160**	**.031**	**393**	**0.075**	**0.046**	**<.001**	**-94.067**
	Participation Coefficient Load - NKI Dataset	-0.095	-0.281	0.090	-0.103	-1.008	.314	393	0.075	0.046	<.001	-94.067

Note: R^2 represents adjusted R^2. AIC = Akaike Information Criterion. HCP = Human Connectome Project rs-fMRI sample. NKI = Nathan Kline Institute- Rockland rs-fMRI sample. Re-parcellation analyses were completed using the Yeo 17-network parcellation scheme to calculate Participation Coefficient.

Table S5.

Iowa Cohort: Hierarchical Linear Regressions with Lesion Volume, Down-sampled Edge Density Load/Peak, and Voxel-wise Participation Coefficient Load/Peak Predicting Post-Lesion g Scores

			Step and Variable	*b*	95% CI for *b* Lower bound	95% CI for *b* Upper bound	β	*t*	*p*	*df*	R^2	ΔR^2	Sig. ΔF	AIC
Raw g Scores	Lesion Load	Model 1	Step 1											
			Total Lesion Volume (log mm^3)	**-0.119**	**-0.179**	**-0.059**	**-0.193**	**-3.926**	**<.001**	**400**	**0.035**	**0.037**	**<.001**	**-80.006**
			Step 2											
			Total Lesion Volume (log mm^3)	0.016	-0.071	0.102	0.025	0.355	.723	398	0.073	0.043	<.001	-94.281
			4mm^3 Edge Density Load	**-0.208**	**-0.391**	**-0.024**	**-0.223**	**-2.223**	**.027**	**398**	**0.073**	**0.043**	**<.001**	**-94.281**
			4mm^3 Participation Coefficient Load	-0.080	-0.271	0.111	-0.085	-0.820	.413	398	0.073	0.043	<.001	-94.281
		Model 2	Step 1											
			Total Lesion Volume (log mm^3)	**-0.120**	**-0.181**	**-0.058**	**-0.188**	**-3.818**	**<.001**	**396**	**0.033**	**0.035**	**<.001**	**-79.304**
			Step 2											
			Total Lesion Volume (log mm^3)	0.005	-0.084	0.094	0.008	0.108	.914	395	0.064	0.033	<.001	-91.078
			4mm^3 Participation Coefficient Load	**-0.248**	**-0.379**	**-0.117**	**-0.267**	**-3.730**	**<.001**	**395**	**0.064**	**0.033**	**<.001**	**-91.078**
		Model 3	Step 1											
			Total Lesion Volume (log mm^3)	**-0.119**	**-0.179**	**-0.059**	**-0.193**	**-3.926**	**<.001**	**400**	**0.035**	**0.037**	**<.001**	**-80.006**
			Step 2											
			Total Lesion Volume (log mm^3)	0.004	-0.078	0.085	0.006	0.089	.929	399	0.074	0.041	<.001	-95.602
			4mm^3 Edge Density Load	**-0.265**	**-0.388**	**-0.141**	**-0.284**	**-4.225**	**<.001**	**399**	**0.074**	**0.041**	**<.001**	**-95.602**
	Lesion Peak		Step 1											
			Total Lesion Volume (log mm^3)	**-0.119**	**-0.179**	**-0.059**	**-0.193**	**-3.926**	**<.001**	**400**	**0.035**	**0.037**	**<.001**	**-80.006**
			Step 2											
			Total Lesion Volume (log mm^3)	0.059	-0.090	0.207	0.095	0.777	.437	398	0.070	0.040	<.001	-93.014
			Lesion Peak 4mm^3 Edge Density	**-0.031**	**-0.045**	**-0.016**	**-0.323**	**-4.123**	**<.001**	**398**	**0.070**	**0.040**	**<.001**	**-93.014**
			Lesion Peak 4mm^3 Participation Coefficient	-0.188	-1.274	0.898	-0.036	-0.340	.734	398	0.070	0.040	<.001	-93.014

g Scores Controlled for Crystallized Intelligence	Lesion Load	Step 1										
		Total Lesion Volume (log mm^3)	**-0.092**	**-0.127**	**-0.058**	**-0.255**	**-5.266**	**<.001**	**400**	**0.063**	**0.065**	**<.001**	**-521.118**
		Step 2											
		Total Lesion Volume (log mm^3)	0.011	-0.038	0.060	0.031	0.447	.655	398	0.128	0.070	<.001	-548.265
		$4mm^3$ Edge Density Load	**-0.123**	**-0.227**	**-0.018**	**-0.225**	**-2.312**	**.021**	**398**	**0.128**	**0.070**	**<.001**	**-548.265**
		$4mm^3$ Participation Coefficient Load	-0.097	-0.205	0.012	-0.177	-1.750	.081	398	0.128	0.070	<.001	-548.265
	Lesion Peak	Step 1											
		Total Lesion Volume (log mm^3)	**-0.092**	**-0.127**	**-0.058**	**-0.255**	**-5.266**	**<.001**	**400**	**0.063**	**0.065**	**<.001**	**-521.118**
		Step 2											
		Total Lesion Volume (log mm^3)	0.034	-0.052	0.120	0.094	0.782	.434	398	0.093	0.023	<.001	-532.512
		Lesion Peak $4mm^3$ Edge Density	**-0.016**	**-0.024**	**-0.007**	**-0.285**	**-3.678**	**<.001**	**398**	**0.093**	**0.023**	**<.001**	**-532.512**
		Lesion Peak $4mm^3$ Participation Coefficient	-0.423	-1.051	0.206	-0.139	-1.321	.187	398	0.093	0.023	<.001	-532.512

Note: R^2 represents adjusted R^2. AIC = Akaike Information Criterion. Four patients had lesions that did not intersect with the participation coefficient map and were thus excluded from Model 2 (N=402).

Table S6. Demographic characteristics of the Iowa and WU cohorts.

Cohort	Iowa (N=402)	WU (N=102)
Age (SD)	58.17 (13.81)	53.29 (11.28)
Sex	212M/190F	58M/44F
Education, years (SD)	13.46 (2.72)	13.32 (2.67)
Handedness	360R/15M/26L	93R/9L
Lesion Chronicity, months (SD)	42.17 (57.58)	0.46 (0.16)
Lesion Laterality	175L/141R/86B	47L/55R

Note: Age and lesion chronicity are measured from date of scan; age is in years; Iowa cohort age range: 20-88; WU cohort age range: 19-83; sex: M=male, F=female; handedness: R=right-handed, L=left-handed, M=mixed-handedness; one participant in the Iowa cohort was missing data on handedness; lesion chronicity is the number of months between date of lesion onset and date of neuroimaging acquisition; lesion laterality: R=right-sided, L=left-sided, B=bilateral. SD=standard deviation

Table S7. Cognitive tests for the Iowa and WU cohorts

Iowa Cohort (N=402)	WU Cohort (N=102)
Wechsler Adult Intelligence Scales:	*Boston Diagnostic Aphasia Examination:*
Block Design	Word Comprehension
Similarities	Complex Ideation
Digit Span	Boston Naming Test
Digit-Symbol Coding	*Wechsler Memory Scales:*
Arithmetic	Spatial Span Forward
Information	Spatial Span Backward
Judgment of Line Orientation Test	*Hopkins Verbal Learning Test:*
Complex Figure Test:	Immediate Recall Total Score
Copy	Delayed Recall
Recall	Discrimination Index
Rey Auditory Verbal Learning Test:	
Immediate Recall Trial 5	
Delayed Recall	
Delayed Recognition Hits	
Trail Making Test:	
Part A	
Part B	
Benton Visual Retention Test	

Table S8.

Iowa Cohort: Hierarchical Linear Regressions with Log-Transformed Lesion Volume and Voxel-wise Functional Connectivity Metrics Predicting Post-Lesion g Scores

Step and Variable	*b*	95% CI for *b*		β	*t*	*p*	*df*	R^2	ΔR^2	Sig. ΔF	AIC
		Lower bound	Upper bound								
Step 1											
Total Lesion Volume (log mm^3)	**-0.119**	**-0.179**	**-0.059**	**-0.193**	**-3.926**	**<.001**	**400**	**0.035**	**0.037**	**<.001**	**-80.006**
Step 2											
Total Lesion Volume (log mm^3)	**-0.070**	**-0.138**	**-0.002**	**-0.113**	**-2.022**	**.044**	**399**	**0.052**	**0.020**	**.004**	**-86.373**
Eigenvector Centrality Load	**-0.162**	**-0.273**	**-0.052**	**-0.162**	**-2.897**	**.004**	**399**	**0.052**	**0.020**	**.004**	**-86.373**
Step 1											
Total Lesion Volume (log mm^3)	**-0.119**	**-0.179**	**-0.059**	**-0.193**	**-3.926**	**<.001**	**400**	**0.035**	**0.037**	**<.001**	**-80.006**
Step 2											
Total Lesion Volume (log mm^3)	-0.003	-0.089	0.082	-0.006	-0.08	.937	399	0.063	0.031	<.001	-91.145
Gateway Centrality Load	**-0.239**	**-0.369**	**-0.11**	**-0.257**	**-3.641**	**<.001**	**399**	**0.063**	**0.031**	**<.001**	**-91.145**
Step 1											
Total Lesion Volume (log mm^3)	**-0.119**	**-0.179**	**-0.059**	**-0.193**	**-3.926**	**<.001**	**400**	**0.035**	**0.037**	**<.001**	**-80.006**
Step 2											
Total Lesion Volume (log mm^3)	-0.024	-0.104	0.057	-0.038	-0.573	.567	399	0.059	0.027	.001	-89.402
Weighted Degree Load	**-0.217**	**-0.342**	**-0.091**	**-0.225**	**-3.387**	**.001**	**399**	**0.059**	**0.027**	**.001**	**-89.402**
Step 1											
Total Lesion Volume (log mm^3)	**-0.119**	**-0.179**	**-0.059**	**-0.193**	**-3.926**	**<.001**	**400**	**0.035**	**0.037**	**<.001**	**-80.006**
Step 2											
Total Lesion Volume (log mm^3)	**-0.113**	**-0.173**	**-0.052**	**-0.183**	**-3.664**	**<.001**	**399**	**0.035**	**0.003**	**.252**	**-79.329**
Within-Module Degree Load	-0.054	-0.146	0.038	-0.057	-1.147	.252	399	0.035	0.003	.252	-79.329

Note: R^2 represents adjusted R^2. AIC = Akaike Information Criterion.

SI References

1. W. J. Schneider, K. S. McGrew, "The Cattell–Horn–Carroll theory of cognitive abilities" in Contemporary intellectual assessment: Theories, tests, and issues, 4th ed. (The Guilford Press, New York, NY, US, 2018), pp. 73-163.
2. P. A. Jewsbury, S. C. Bowden, K. Duff, The Cattell–Horn–Carroll Model of Cognition for Clinical Assessment. *Journal of Psychoeducational Assessment* **35**, 547-567 (2017).
3. D. Wechsler, *WAIS-IV Technical and Interpretive Manual* (Pearson, 2008).
4. G. Wilkerson, G. Robertson, WRAT4 wide range achievement test professional manual. *Lutz, FL: Psychological Assessment Resources* (2006).
5. M. Mitrushina, K. B. Boone, J. Razani, L. F. D'Elia, *Handbook of normative data for neuropsychological assessment* (Oxford University Press, 2005).
6. S. v. Buuren, K. Groothuis-Oudshoorn, mice: Multivariate imputation by chained equations in R. *Journal of statistical software*, 1-68 (2010).
7. R. C. Team, R: A Language and Environment for Statistical Computing. (2013).
8. K. A. Bollen, M. D. Noble, Structural equation models and the quantification of behavior. *Proceedings of the National Academy of Sciences* **108**, 15639-15646 (2011).
9. M. Muthukrishna, J. Henrich, A problem in theory. *Nature Human Behaviour* **3**, 221-229 (2019).
10. Y. Rosseel, Lavaan: An R package for structural equation modeling and more. Version 0.5–12 (BETA). *Journal of statistical software* **48**, 1-36 (2012).
11. L. t. Hu, P. M. Bentler, Cutoff criteria for fit indexes in covariance structure analysis: Conventional criteria versus new alternatives. *Structural Equation Modeling: A Multidisciplinary Journal* **6**, 1-55 (1999).
12. R. B. Kline, *Principles and Practice of Structural Equation Modeling, Fourth Edition* (Guilford Publications, 2015).
13. J. R. Crawford, "Estimation of Premorbid Intelligence: A Review of Recent Developments" in Developments in Clinical and Experimental Neuropsychology, J. R. Crawford, D. M. Parker, Eds. (Springer US, Boston, MA, 1989), 10.1007/978-1-4757-9996-5_6, pp. 55-74.
14. D. R. Orme, B. Johnstone, R. Hanks, T. Novack, The WRAT-3 Reading Subtest as a Measure of Premorbid Intelligence Among Persons With Brain Injury. *Rehabilitation Psychology* **49**, 250-253 (2004).